RSC Advances

ROYAL SOCIETY OF CHEMISTRY

www.rsc.org/advances

Copper-Cobalt Synergy in $Cu_{1-x}Co_xFe_2O_4$ Spinel Ferrite as a Highly Efficient and Regioselective Nanocatalyst for Synthesis of 2,4-Dinitrotoluene

Reza Fareghi-Alamdari*[a],Farzad Zandi[a], Mohammad Hossein Keshavarz[b]

a) College of Chemistry and Chemical Engineering, Malek-Ashtar University of Technology, Tehran, 16765-3454, I. R. Iran

b) Department of Chemistry, Malek-Ashtar University of Technology, Shahin-Shahr, 83145-115, I. R. of Iran

Email: reza_fareghi@yahoo.com, Tel: +982122970277, Fax: +982122970195

Abstract

Highly regioselective dinitration of toluene with nitric acid as nitrating agent in the presence of $Cu_{1-x}Co_xFe_2O_4$ ($0 \leq x \leq 1$) as nanocatalysts is described. The results of this protocol show that this nitration system can significantly improve the selectivity and the yield of 2,4-dinitrotoluene. The prepared spinel ferrites were characterized by scanning electron microscopy (SEM), energy dispersive X-ray spectroscopy (EDX), X-ray diffraction (XRD), and Fourier transform infrared spectroscopy (FT-IR). Copper and cobalt synergy (50%:50%) in spinel ferrite also shows the best catalytic activity in the selectivity of dinitrotoluene under solvent-free conditions.

Keywords: Nitration, Dinitrotoluene, Regioselective, Spinel ferrite, Solvent-free

1. Introduction

Nitration of toluene is a very important process in the production of different chemical commodities which is usually carried out using nitric and sulfuric acids on a large volume scale. [1, 2] The use of less hazardous chemicals, safer solvents and auxiliaries are very important topics in chemical industries towards introducing environmentally benign chemical processes. There have been some recent efforts in this regard, for example by replacing the sulfuric acid with heterogeneous catalysts and carrying out the reaction in a safer solvent. 2,4-Dinitrotoluene (2,4-DNT) is a significant product and a crucial intermediate for the production of many industrially important materials including explosives, and propellants, [3] dyes, [4] polyurethanes, [5, 6] pharmaceuticals, [7] agrochemicals, [8] and fragrances [9]. As previously mentioned, 2,4-DNT is employed in double based propellants as a plasticizer, and the existence of impurities in 2,4-DNT can lead to mechanical and safety problems. Therefore, the high purity of 2,4-DNT is an important requirement in the production of this material. 2,4-DNT is produced annually on a scale of many million metric tons worldwide and mostly converted to tolylene diisocyanate, i.e. an important and necessary precursor to polyurethane resins employed for rigid and flexible foams, coatings, elastomers, and fibers. [10] Unfortunately, the process of dinitration of toluene with nitric and sulfuric acids (mixed acid) produces 2,4- , and 2,6-dinitrotoluenes (2,6-DNT) in a ratio of only four to one (4:1). [11] However, separation of 2,4-DNT from 2,6-DNT is a difficult and expensive work. In addition, the use of sulfuric acid for generation of nitronium ions is a contributor to environmentally harmful waste. In recent years, major endeavors are therefore being made to develop environmentally, friendly, safe, and clean benign processes, especially for the regioselective *para*-substituted products in dinitrotoluene. [10, 12-15]

On the other hand, it is well recognized that mesoporous catalysts can display an important role through their ability to act as reusable heterogeneous catalysts which can increase product selectivities. [16-18] Furthermore, they can be easily separated from the reaction mixtures by simple filtration and reused several times to give the same selectivity and yield. Most studies in this field have focused on the application of regioselective heterogeneous catalysts between a precursor nitronium ion and a benzene ring. There have been several attempts to improve the selectivity of nitration of toluene using heterogeneous catalysts. [19-22] In the process of classical nitration based on nitric and sulfuric acids or phosphoric mixed acids, the 2,4-DNT and 2,6-DNT isomers were obtained in approximately a 4:1 ratio. [23] 2,4-DNT is a main and basic chemical commodity of great market demand. After the original work by Othmer and co-workers [24] in 1944, further progress for nitration of aromatic compounds was achieved by Adamiak and co-worker, [25] Gao et al., [26] Liu et al., [27] and Green et al. [28] in the recent years. For example, in 2011, Lu and co-worker [20] reported regioselective nitration of different aromatic rings such as toluene, ethylbenzene and etc using N_2O_5 in the presence of ionic liquid. However, in this study, the reaction carried out in CCl_4 which is a hazardous solvent. Moreover, conversion of reactants to products can give moderate to good yields (61.3-89.9%). In another study in 2013, the Smith's group [29] reported the application of zeolite Hβ in dinitration of toluene. In this research, the mono substituted toluene using propanoic anhydride was obtained along with 2,4-DNT and 2,6-DNT. Hence, so far there exists no general and highly regioselective catalytic systems for production of 2,4-DNT with good selectivity and yield

Due to specific chemical and physical properties of spinel ferrites, there have been several endeavors to investigate their mechanisms. [30, 31] They are widely employed in gas sensor, [32] electrode materials, [33] adsorption, [34] and catalysis. [35, 36] Ternary and binary spinel ferrites such as

$Mg_{1-x}Co_xFe_2O_4$, [37] $Co_{0.2}Cu_{0.03}Fe_{2.77}O_4$, [38] $Cu_{1-x}Co_xFe_2O_4$, [39-41] $Pr_xCoFe_{2-x}O_4$,[42] $ZnFe_2O_4$, [43] $NiFe_2O_4$, [44] $MnFe_2O_4$, [45] $CoFe_2O_4$, [46, 47] and $CuFe_2O_4$ [48] have been reported to display better catalytic and electrochemical performance than single component metal oxides due to their achievable oxidation state and specific structure. The ternary and binary spinel ferrites also have some application in organic synthesis. Recently, Ghahramanzadeh and co-workers reported the application of $MnFe_2O_4$ nanoparticles as a magnetic nanocatalyst for the synthesis of spirooxindoles in water. [49] In addition, the $Cu_{1-x}Co_xFe_2O_4$ was employed in the synthesis of different dibenzoxanthenes under solvent free conditions. [35]

As shown in Figure 1, different products of the nitration of toluene are described. Distribution of different products depends on various parameters, e.g. the molar ratio of toluene to nitric acid, temperature of the reaction, type of catalyst and solvent. Due to the presence of desired physic-chemical properties of ternary spinel ferrites especially $Cu_{1-x}Co_xFe_2O_4$, the spinel ferrites $Cu_{1-x}Co_xFe_2O_4$ are used for regioselective and green synthesis of 2,4-DNT in this study.

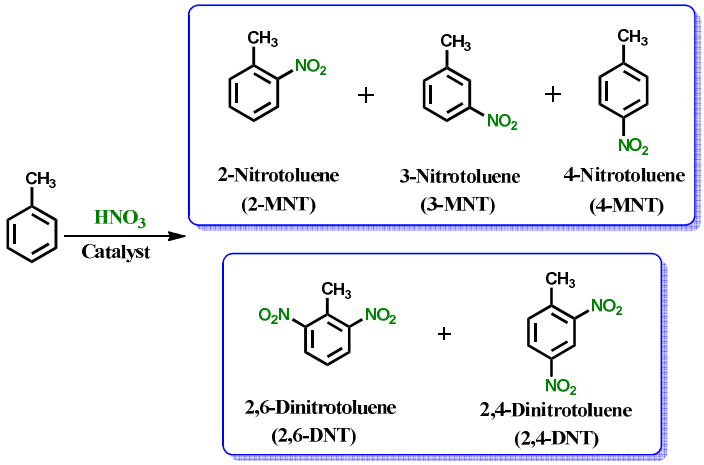

Figure 1. Different products for nitration of toluene in the presence of spinel ferrites

2.Experimental

2.1. Materials and apparatus

Toluene and nitric acid were purchased from Merck chemical company. All of the used solvents and $FeCl_3.6H_2O$, $CoCl_2.6H_2O$, $CuCl_2.2H_2O$, and hexadecyltrimethylammonium bromide (CTAB) were purchased from Merck, and Fluka chemical companies. FT-IR spectra were obtained with KBr pellets in the range of 400-4000 cm^{-1} with FT-IR Shimadzu-8776 spectrometer. X-ray diffraction (XRD) patterns were recorded by the X-ray diffractometer (Philips PW-1800). The particle size and external morphology of the fine calcined powders were characterized by scanning electron microscopy (SEM) (Philips XL30). All samples were coated with gold at 10 m.A. for 2 min prior to SEM analysis. Energy dispersive X-ray spectroscopy (EDX) analysis was studied by Philips XL30 microscope.

2.2. *Analysis and characterization of the products*

Analysis of the products was carried out by gas chromatography (GC) with these specifications: (i) Column: CP-SIL 8CB, L=25 m, d= 0.32 mm, film=1.20 μm; (ii) Inlet: injector (1079) 250 °C; (iii) Split injection; (iv) Injected volume: 0.1 μL; (v) Carrier gas: N_2; (vi) Pre-column pressure: 50 kPa; (vii) Oven: 160 °C (3 min) with 20 °C/min; (viii) Isotherm 180 °C (30 min); (ix) Detector: FID; (x) Integration: Varian CP-3800; and (xi) Internal standard: *para*-nitroacetophenone. All of the expected final products from the nitration of toluene were purchased from Aldrich Chemical Company in order to determine response factors and retention times relative to ethyl acetate for each product.

2.3. Preparation of $M_{1-x}M'_xFe_2O_4$ with different molar ratio of copper and cobalt

First, 1.0 g of CTAB was dissolved in 35 mL of deionized water. Later, 1.0 g of $FeCl_3.6H_2O$ was added to the beaker and it was stirred for 10 min (**S1**). Then, the appropriate amounts of $CuCl_2.2H_2O$ and $CoCl_2.6H_2O$ salts according to Table 1 were dissolved in deionized water (**S2**). **S2** was added by a burette into **S1** (**S3**). After that, an aqueous solution of NaOH (5 M) was introduced drop-wise into the **S3** solution (*pH*= 10-11). The mixture was also stirred for 30 min. The resultant materials were transferred into an autoclave (L= 7.3 cm, D= 3.9 cm). The autoclave was kept at 160°C for 72 h. After three days, the autoclave was allowed to cool down slowly to room temperature. The desired $Cu_{1-x}Co_xFe_2O_4$ ($0 \leq X \leq 1$) was washed several times with deionized water and dried at room temperature.

Table 1. The amount of starting materials for the preparation of $Cu_{1-x}Co_xFe_2O_4$ ($0 \leq X \leq 1$) spinel ferrite nanocatalysts.

Entry	X	$Cu_{1-x}Co_xFe_2O_4$	$CoCl_2.6H_2O$ (g)	$CuCl_2.2H_2O$ (g)	$FeCl_3.6H_2O$ (g)	CTAB (g)
1	0	$CuFe_2O_4$	0	0.32	1.0	1.0
2	0.25	$Cu_{0.75}Co_{0.25}Fe_2O_4$	0.11	0.24	1.0	1.0
3	0.5	$Cu_{0.5}Co_{0.5}Fe_2O_4$	0.22	0.16	1.0	1.0
4	0.75	$Cu_{0.25}Co_{0.75}Fe_2O_4$	0.33	0.079	1.0	1.0
5	1	$CoFe_2O_4$	0.44	0	1.0	1.0

2.4. Typical procedure for dinitration of toluene using nitric acid over $Cu_{0.5}Co_{0.5}Fe_2O_4$ under solvent-free conditions

First, in a 25 mL round bottom two-neck flask equipped with a magnetic bar and condenser, 0.09 g (0.37 mmol) of $Cu_{0.5}Co_{0.5}Fe_2O_4$ and 0.32 g (5 mmol) of 98%nitric acid were added and heated at 90 °C for 10 min. Then, 0.23 g (2.5 mmol) of toluene was added to the reaction mixture and stirred at 90 °C for 4 h. The progress of the reaction was monitored by thin layer chromatography

(TLC) (*n*-hexane/EtOAc 9:1). After completion of the reaction, the reaction mixture was slowly cooled to room temperature as well as 25 mL of EtOAc was added and stirred. Then, the reaction mixture was filtered over sinter glass (G-4) under reduced pressure. Finally, for separation and isolation of the pure product of 2,4-DNT from mononitrotoluene, the reaction mixture was recrystallized in ethanol. The isolated yield and melting point of 2,4-DNT were 88% and 69-71 °C, respectively. In addition, the pure product was identified by ^{1}H NMR, ^{13}C NMR, and FT-IR spectroscopy.

2,4-Dinitrotoluene; IR (KBr): ν (cm^{-1}) 3087, 3057, 2870, 1608, 1531, 1479, 1466, 1445, 1383, 1270, 1164, 1036, 843, 836, 791, 637, ^{1}H NMR (400 MHz, $CDCl_3$/TMS) δ(ppm): 2.38 (3H, s, Me), 7.54 (1H, d, *J=7.8 Hz*, Ar), 8.08 (1H, d, *J=7.8 Hz*, Ar), 8.65 (1H, s, Ar), ^{13}C NMR (100 MHz, $CDCl_3$/TMS) δ(ppm): 20.48, 120.16, 127.05, 134.55, 141.01, 146.58, 149, 19.

3. Results and Discussion

3.1. Preparation of $Cu_{1-x}Co_xFe_2O_4$

As shown in Figure 2, $Cu_{1-x}Co_xFe_2O_4$ spinel ferrites were prepared in four steps, which give five spinel ferrite nanocatalysts with different molar ratios of copper and cobalt. Undoubtedly, the synergy of copper and cobalt displays the best catalytic performance, cubic shape, and overall yield of products. [50, 51]

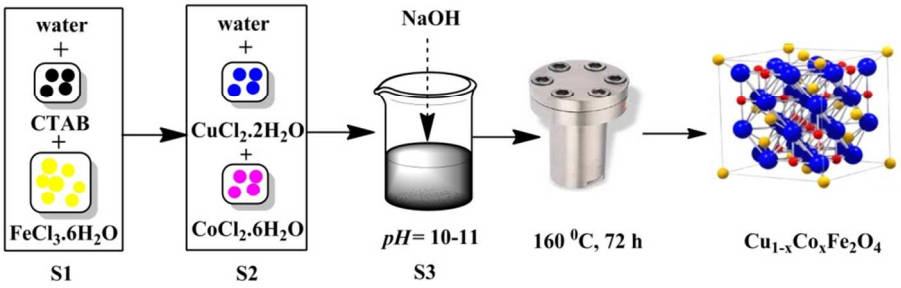

Figure 2. Synthetic route for the preparation of different spinel ferrites

3.2. Characterization of $Cu_{1-x}Co_xFe_2O_4$

3.2.1. XRD analysis

XRD patterns of the $CuFe_2O_4$, $Cu_{0.5}Co_{0.5}F_2O_4$, and $CoFe_2O_4$ are displayed in Figure 3. They revealed the presence of (220), (311), (400), (422), (511) and (440) major lattice plane for the cubic spinel phase with Fd_3m space group. Clear lattice plane of (111) and (422) is also present. These results confirmed the presence of only one spinel phase without any significant impurities. $CuFe_2O_4$ spinel ferrite shows various patterns due to cubic spinel phase and a considerable amount of CuO and Fe_2O_3 (Figure 3a). Substitution of copper with cobalt increases the overall crystallinity of the spinel phase. XRD pattern of $CoFe_2O_4$ (Figure 3c) revealed the formation of single phase cubic spinel structure with a sharp peak attributed to (311) reflection, which indicates that the crystallites are preferentially oriented along the (311) plane. The breadth of the Bragg peak is a combination of both instrument and sample dependent effects. To decouple these contributions, it is necessary to collect a various pattern from the line broadening of a standard material such as silicon for determination of the instrumental broadening. The corrected instrumentation broadening β corresponding to the diffraction peak of $Cu_{1-X}Co_xFe_2O_4$ (x=0.0, 0.5 and 1.0) was estimated by using the below equation:

$$\beta = \beta_1 - \beta_2 \qquad (1)$$

The crystallite sizes (D_c) of $Cu_{1-x}Co_xFe_2O_4$ spinel ferrite were calculated by using the Debey–Scherrer equation (Table 2):

$$D_c = \frac{K\lambda}{\beta \cos\theta} \qquad (2)$$

Where β is the breadth of the observed diffraction peak at its half-intensity maximum; K is the so-called shape factor, which usually takes a value of about 0.9; and λ is the wavelength of X-ray source used in XRD instrument.

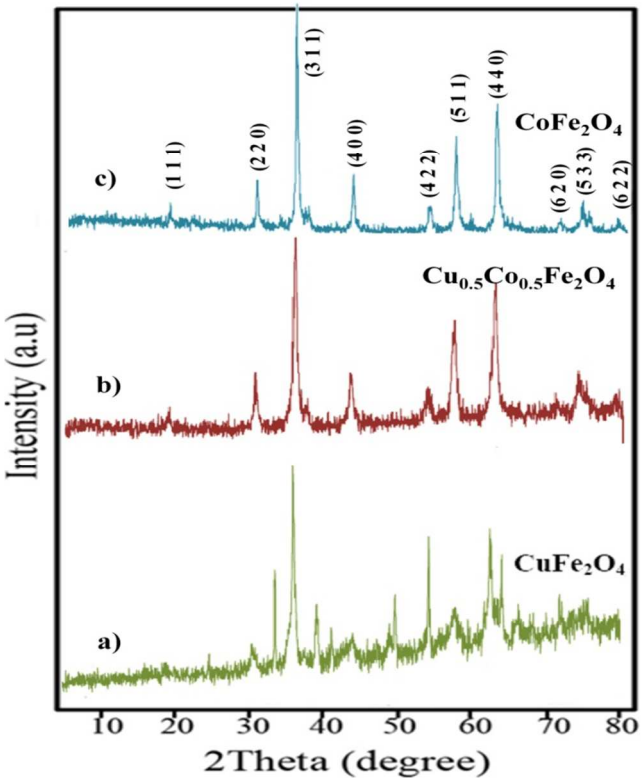

Figure 3. XRD pattern of a) $CuFe_2O_4$ b) $Cu_{0.5}Co_{0.5}Fe_2O_4$ c) $CoFe_2O_4$

The information of XRD patterns, such as FWHM, and XRD diffraction data of $Cu_{1-X}Co_xFe_2O_4$ for the most intense reflection, are presented in Table 2. As shown from these data, the crystallite sizes of $CuFe_2O_4$, $Cu_{0.5}Co_{0.5}Fe_2O_4$, and $CoFe_2O_4$ were 18, 22, and 20 nm, respectively.

Table 2. Crystalline size of spinel ferrites $Cu_{1-X}Co_xFe_2O_4$ according to XRD patterns.

Entry	X	$Cu_{1-X}Co_xFe_2O_4$	2θ(deg)	FWHM(deg)	D (nm)
1	0	$CuFe_2O_4$	35.4	0.24372	18
2	0.5	$Cu_{0.5}Co_{0.5}Fe_2O_4$	35.4	0.32946	22
3	1	$CoFe_2O_4$	35.2	0.32755	20

3.2.2. FT-IR study

Figure 4 shows the FT-IR spectra of $CuFe_2O_4$, $Cu_{0.5}Co_{0.5}Fe_2O_4$, $Cu_{0.25}Co_{0.75}Fe_2O_4$, and $CoFe_2O_4$ spinel ferrite. Two important broad bands of metal–oxygen are observed in all of the spinel, especially spinel ferrites. The value of ν_1, generally the highest one, was observed in the range of 550-600 cm^{-1}, which corresponds to the intrinsic stretching vibrations of the metal at the tetrahedral site, [$M_{tetra}\leftrightarrow O$]. Whereas the lowest band (ν_2) was observed in the range of 450–385 cm^{-1}, which is related to octahedral metal stretching [$M_{octa}\leftrightarrow O$]. Since no clear peak attributed to octahedrally coordinate metal ions has been observed, detection limit of our FT-IR instrument is expected to be less than 400 cm^{-1}. The bands within about 2845-2923 cm^{-1} and 1060-1120 cm^{-1} are related to stretching modes of C–H and C–O groups, respectively. The broad band centered about 3430 cm^{-1} can be assigned to O–H stretching mode for arising from the surface hydroxyl groups on the spinel ferrite. The absorption band at 1630 cm^{-1} on spectra refers to the vibration of remaining H_2O in the sample.

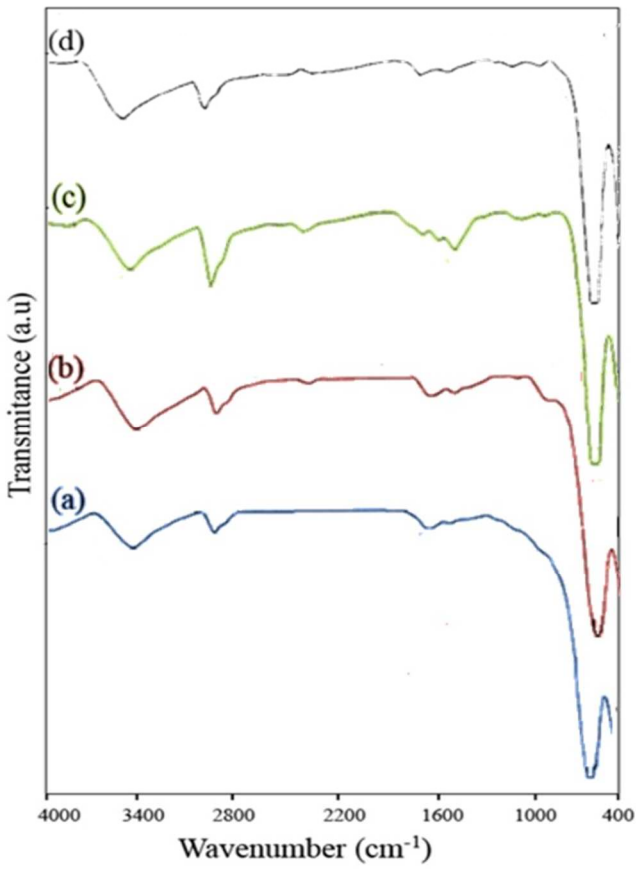

Figure 4. FT-IR spectra of a) $CuFe_2O_4$ b) $Cu_{0.5}Co_{0.5}Fe_2O_4$ c) $Cu_{0.25}Co_{0.75}Fe_2O_4$ d) $CoFe_2O_4$

3.2.3. SEM and EDX studies

The morphologies of the spinel ferrites were investigated by SEM micrograph that is shown in Figure 5. SEM images were employed to observe the grain microstructure of the nanoparticles, which would provide a better view of the grain development and grain sizes. These figures indicate that the prepared spinel ferrites were obtained by the hydrothermal method as being uniform in both morphology and crystalline size. As shown in Figure 5a, the cubic morphology was observed for $Cu_{0.5}Co_{0.5}Fe_2O_4$. As can be seen from SEM images, grains have different morphologies other than spherical. A broad size distribution is observed, which consists of

nearly octahedral crystals with an average size of about 30 nm. The calculated grain sizes of $Cu_{1-x}Co_xFe_2O_4$ (x= 0, 0.25, 0.50, 0.75 and 1) are 48, 34, 26, 24, and 29 nm, respectively.

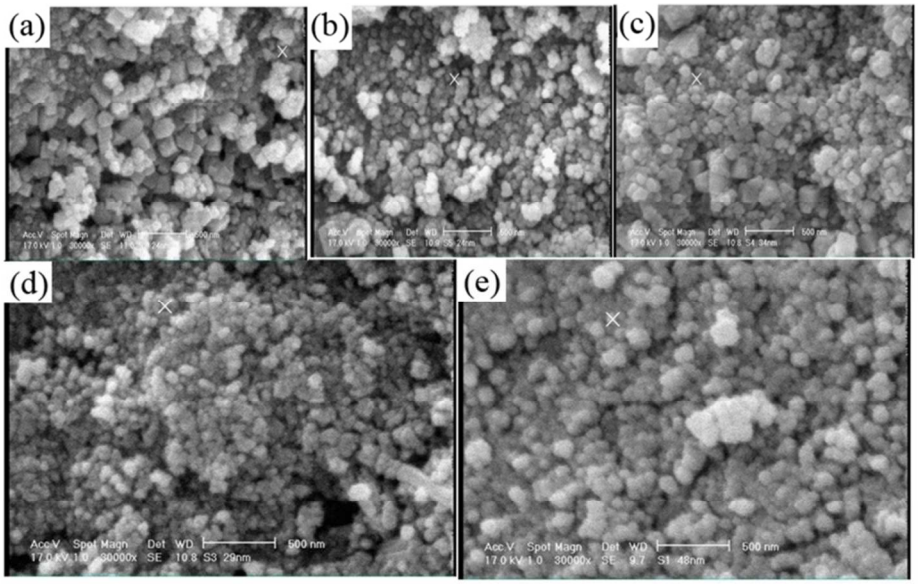

Figure 5. SEM micrograph of a) $Cu_{0.5}Co_{0.5}Fe_2O_4$ b) $Cu_{0.25}Co_{0.75}Fe_2O_4$ c) $Cu_{0.75}Co_{0.25}Fe_2O_4$ d) $CoFe_2O_4$ e) $CuFe_2O_4$

In addition, the distributions of grain size of spinel ferrites are obtained in every prepared catalyst, and histograms of the average size of spinel ferrites based on percentage of particles are depicted in Figure 6. The main percentage of distribution of nanoparticles is nearly predicted by SEM, and XRD patterns. For example in the spinel ferrite $Cu_{0.5}Co_{0.5}Fe_2O_4$, 69% of nanoparticles are at approximately 26 nm. For other spinel ferrites such as $Cu_{0.25}Co_{0.75}Fe_2O_4$, $Cu_{0.75}Co_{0.25}Fe_2O_4$, $CoFe_2O_4$, and $CuFe_2O_4$, the main particle sizes are also (74%, 24 nm), (68%, 34nm), (64%, 24 nm), and (55%, 48 nm), respectively.

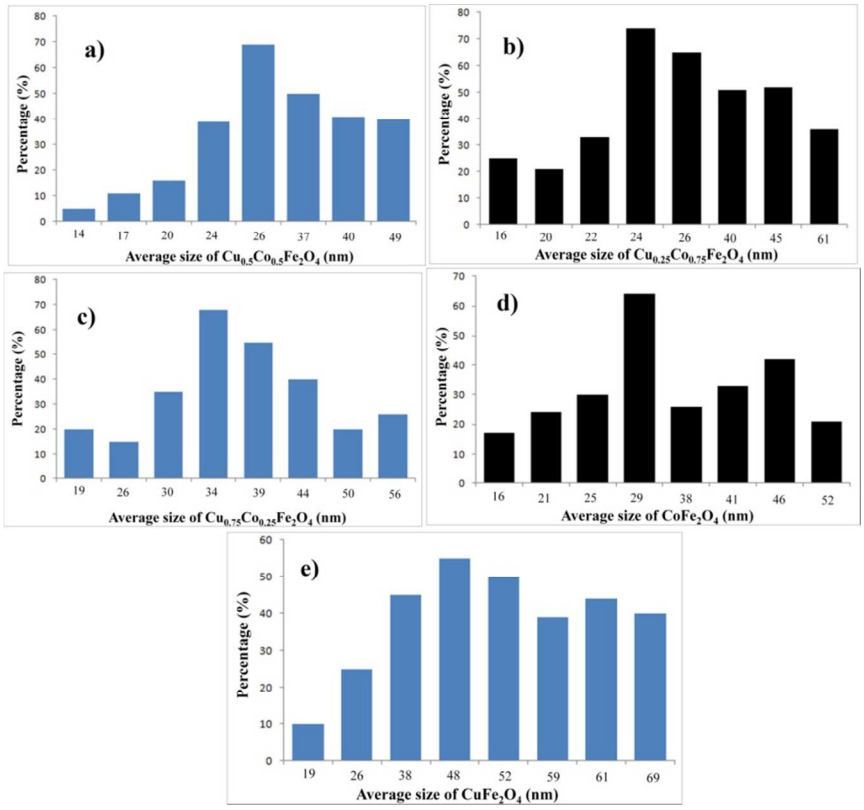

Figure 6. Distribution of particle sizes of prepared catalysts according to SEM images

EDX was used for further clarify the existence of iron (Fe), copper (Cu), and cobalt (Co) ions and briefly understand the information about the chemical composition of the resultant nanosized spinel ferrites. The resultants of numeric analysis are given in Table 3. Moreover, EDX spectra of the $Cu_{0.5}Co_{0.5}Fe_2O_4$, and $CoFe_2O_4$ are shown in Figure 7. EDX spectra indicate the presence of 0.5 of Cu and 0.5 of Co for $M_{1-x}M'_xFe_2O_4$ (Figure 7a). They also show the existence of the other elements such as Fe, and O, which exist in the catalyst. As shown in Figure 6b, although the presence of the element of Co is confirmed, there is no evidence for the existence of Cu in the spectrum.

Table 3. The EDX analysis results of $Cu_{0.5}Co_{0.5}Fe_2O_4$, and $CoFe_2O_4$

Entry	Catalyst	Fe Wt.%	Co Wt.%	Cu Wt.%
1	$CoFe_2O_4$	65.70	34.30	0
2	$Cu_{0.5}Co_{0.5}Fe_2O_4$	63.49	18.26	18.25

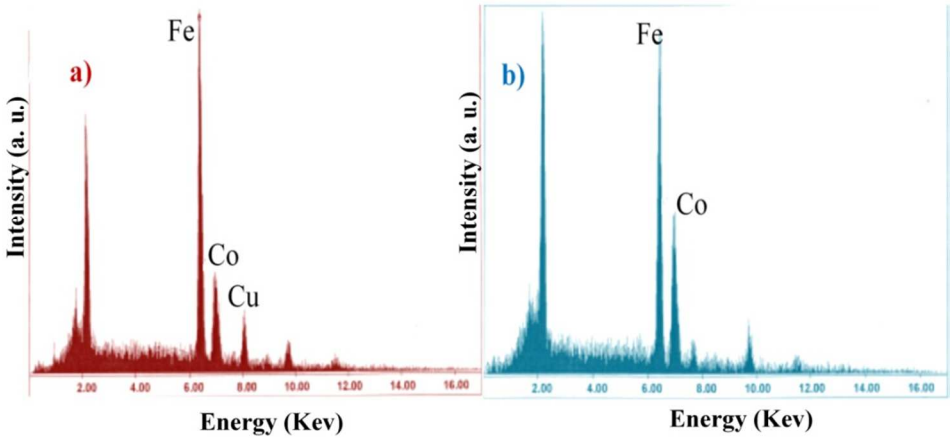

Figure 7. EDX of a) $Cu_{0.5}Co_{0.5}Fe_2O_4$ b) $CoFe_2O_4$

3.3. Catalytic evaluation of $Cu_{1-x}Co_xFe_2O_4$ spinel ferrites in the dinitration of toluene

Different experiments were used with toluene and nitric acid as nitrating agent in the presence of $Cu_{1-x}Co_xFe_2O_4$ for dinitration of toluene in order to obtain the most appropriate conditions such as type of the catalyst, medium and temperature of the reaction, the amount of the catalyst, the molar ratio of the reactant on the selectivity and overall yield of the reaction. Since toluene is moderately activated compound by the methyl group in which the dinitration of toluene occur on active ring, the initial step of nitration of toluene is mostly complete and the second nitration needs hard conditions.

3.3.1. The effect of different spinel ferrites on nitration of toluene

The reactions were carried out in the presence of different spinel ferrites and all of the results were depicted in Figure 8. As shown in this Figure, the binary spinel ferrite $CuFe_2O_4$ was used in this reaction. The yields of 2-nitrotoluene (2-MNT), 4-nitrotoluene (4-MNT), and 2,4-DNT were 35.1%, 15.1%, and 49.8%, respectively. In this experiment, the isomer 2,6-DNT was obtained in trace amount so that the structure and shape of prepared catalysts did not allow the formation of two nitro groups in the vacant adjacent of methyl group of toluene. [52] Meanwhile, the binary spinel ferrites $CuFe_2O_4$ preferred the formation of 2-MNT as compared to 4-MNT (ratio: 2.3). Furthermore, in accordance to SEM image of Figure 5a, $CuFe_2O_4$ has sphere-like shape. Since, the sphere shape in spinel ferrite deals with the formation of 2-MNT and 4-MNT, little amount of the desired product 2,4-DNT was formed by using cubic shape of spinel ferrite. Moreover, the other binary spinel ferrite $CoFe_2O_4$ prefers the formation of *ortho*-isomer relative to *para*-isomer too (ratio: 3.35). Two binary spinel ferrites $CuFe_2O_4$, and $CoFe_2O_4$ show low activity for the formation of the main product (2,4-DNT). Meanwhile, the fifty-fifty synergy between two metals in the structure spinel ferrite can increase the yield of 2,4-DNT to 78.9%.

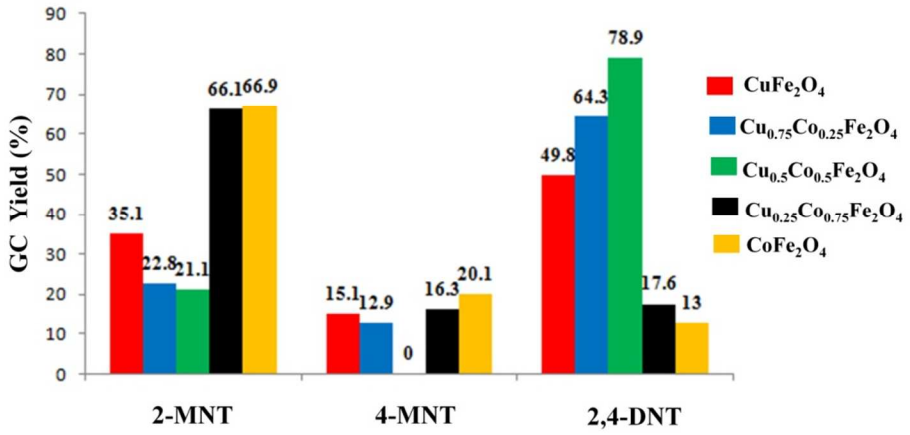

Figure 8. The influence of different prepared binary and ternary spinel ferrites on the nitration of toluene. (Reaction conditions: toluene: HNO_3, 98%: $Cu_{1-x}Co_xFe_2O_4$= 1:2:0.15, solvent: *n*-hexane, T= reflux, time= 4h)

Retention times of ethyl acetate (solvent), 2-MNT, 4-MNT, 4-nitroacetophenone (internal standard) and 2,4-DNT were 1, 3.3, 3.8, 7.0, and 9.2 min, respectively. Figure 9 shows the GC chromatogram of reaction mixture for previous experiment (green legend) that has been used for determination of different isomers of mono and dinitrotoluene. As shown in this Figure, the peak about 1 min is related to ethyl acetate as solvent. In 3.2 min the peak of 2-MNT was revealed and at about 3.8 min the peak of 4-MNT did not appear. Also, the peaks at 7.0 and 9.18 min are related to internal standard and 2,4-DNT respectively.

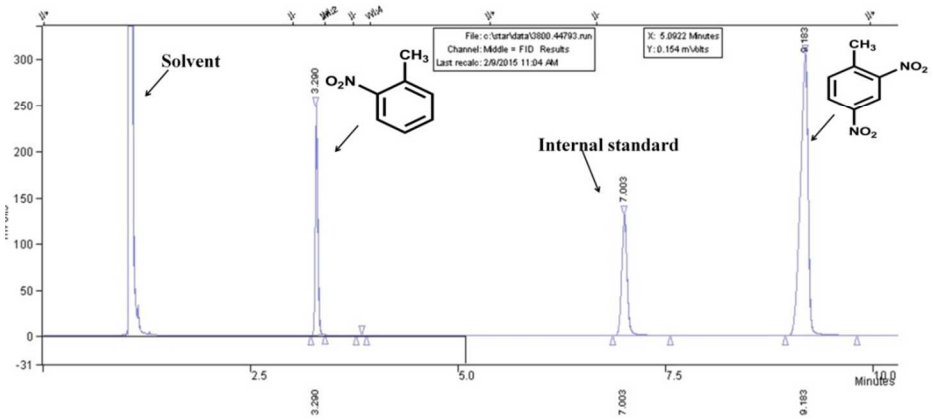

Figure 9. GC chromatogram (Reaction conditions: toluene: HNO_3 98%: $Cu_{0.5}Co_{0.5}Fe_2O_4$= 1:2:0.15, solvent: *n*-hexane, T= reflux, time= 4h, internal standard: 4-nitroacetophenone)

3.3.2. The effect of solvent on the nitration of toluene

In order to check the effect of solvent on the nitration of toluene, the reactions were carried out in five organic solvents, i.e. *n*-hexane, CH_2Cl_2, CH_3OH, EtOAc and CH_3NO_2, and also solvent-free conditions. As shown in Figure 10, the five different solvents of varied polarity employed in which *n*-hexane with a low dielectric constant displayed the best results. For *n*-hexane with boiling point 68 °C, the progress of the reaction was slow. In accordance to the plausible mechanism, the first stage of this reaction is the formation of nitronium ion. Therefore, for providing the activation energy, high temperature of the reaction medium accelerate the formation of nitronium ion that can influence on the selectivity, distribution and yield of the products. The solvent-free conditions exhibited the best yield for 2,4-DNT (90.9%). The isomer 4-MNT did not form under this condition. However, high temperature improves the selectivity and the rate of formation of nitronium ion, which are important for the formation of isomer 2,4-DNT. The formation of 2,4-DNT was decreased by increasing in dielectric constant of the used solvents. According to the plausible mechanism, the solvated nitronium ions by polar solvents

can affect the direction and approach of the substrates. However, the use of polar solvents can decrease the yield of 2,4-DNT. [10] Therefore, the addition of organic solvent to the nitration system has no benefit on either selectivity or yield of the reaction.

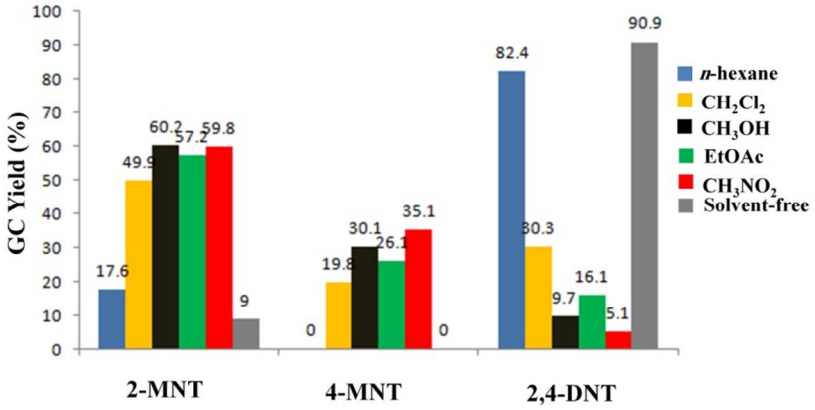

Figure 10. Effect of different solvent in the dinitration of toluene (Reaction conditions: toluene: HNO_3 98%: $Cu_{0.5}Co_{0.5}Fe_2O_4$= 1:2:0.15, time= 4h)

3.3.3. The effect of temperature and concentration of nitric acid on the nitration of toluene

The influence of temperature on dinitration of toluene, and concentration of nitric acid were tabulated in Table 4. As shown in Table 4, two different concentrations of nitric acid (65% or 98%) were used at various temperature of the reaction (r.t. to 90 °C). The products of 2-MNT, 4-MNT, and 2,4-DNT were produced in 56.0%, 35.0%, and 8.8% respectively for 6 h under solvent-free conditions by using 65% nitric acid at room temperature (Table 4, entry1) for which, the yield of 2,4-DNT was very low (8.8%). Two important reasons exist for this situation: (1) low concentration of nitric acid (65 %) can cause the protonation of other molecules of nitric acid; and (2) the low temperature of the reaction was not sufficient for the second nitration on *para*-position of toluene. However, when the temperature of the reaction was increased to 90 °C,

the reaction gave 34.8% of 2-MNT, 22.7% of 4-MNT, and 42.5% of 2,4-DNT for 4h in the presence of $Cu_{0.5}Co_{0.5}Fe_2O_4$ under solvent-free conditions (Table 4, entry 4).

Concentration of nitric acid was improved to 98% in order to achieve high yields of 2,4-DNT, which correspond to entries 5-9 of Table 4. For entry 5 of Table 4, the yield of 2,4-DNT was 10.3%, that gives only 1.5% higher yield relative to the same conditions for 65% nitric acid. Therefore, the effect of temperature is important, which was revealed with two tests (Table 4, entries 1 and 5). The reactions were checked at different temperatures 60, 80, 90, and 100 °C by using 98% nitric acid. The best result was obtained at T = 90 °C in which the yields of 2-MNT, 4-MNT, and 2,4-DNT were 9.7, trace, and 90.2 %, respectively.

Table 4. Effect of temperature on dinitration of toluene with HNO_3 in the presence of $Cu_{0.5}Co_{0.5}Fe_2O_4$.

Entry	HNO_3 (%)	T (^oC)	Time (h)	2-MNT (%)[a]	4-MNT (%)[a]	2,4-DNT (%)[a]
1	65	r.t.	6	56.0	35.0	8.8
2	65	60	6	52.3	19.2	28.5
3	65	80	4	39.8	25.4	34.8
4	65	90	4	34.8	22.7	42.5
5	98	r.t.	5	52.3	37.2	10.3
6	98	60	4	39.2	24.8	36.0
7	98	80	4	28.0	21.5	50.5
8	98	90	1	9.7	0	90.2
9	98	100	1	37.9	18.0	44.0

[a]: GC Yields.

3.3.4. The effect of amount of the catalyst on the nitration of toluene

Mole percent of catalyst is defined as (mmol catalyst/mmol toluene)×100 to check an improvement of the yield and selectivity even further, which can change from 10 to 40 mol%. All of the results were depicted in Figure 11. As shown in this Figure, 15 mol% of $Cu_{0.5}Co_{0.5}Fe_2O_4$ gave the best result with the production of 9.7% 2-MNT, 90.2% 2,4-2DNT, and

trace amount of 4-MNT. The main product of reaction was produced lower than 90% by increasing in catalytic amount of $Cu_{0.5}Co_{0.5}Fe_2O_4$. High amount of catalyst caused that the effective collisions between substrates were decreased and the best catalytic activity did not exhibit.

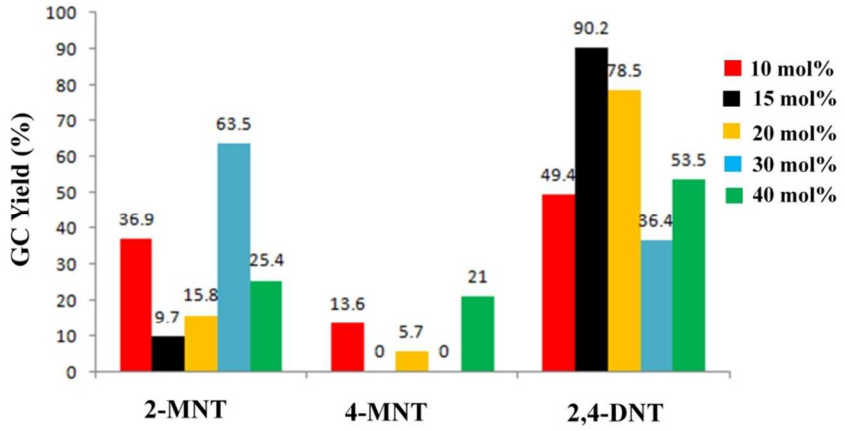

Figure 11. Effect of catalyst amount in dinitration of toluene (Reaction conditions: Toluene: 98% HNO_3= 1:2, T= 90 °C, solvent-free, time= 4h)

3.3.5. The effect of different molar ratio of toluene: nitric acid

Reactions were also conducted in different molar ratio of toluene: 98% nitric acid so that the results were shown in Figure 12. As can be seen from Figure 12, with the molar ratio of 1:1 of substrates, the product 2,4-DNT was only produced in 7.1%. Meanwhile, the best result was obtained in 90.4% of 2,4-DNT and 9.5% of 2-MNT with the molar ratio of 1:2. In molar ratio 1:1, the ratio of *ortho* / *para* was 4.3. This ratio in molar ratio of 1:2 was the best and successful result because 4-MNT did not produce. With increasing in molar ratio of toluene: nitric acid, the yield of 2,4-DNT was decreased from 90.4% to 24.1% in molar ratio of 1:5. It is not clear whether decreasing in 2,4-DNT was real as a result of production of 2,4,6-trinitrotoluene, which

would not have been detected by the used GC system, or whether the results reflect experimental error in the measurements.

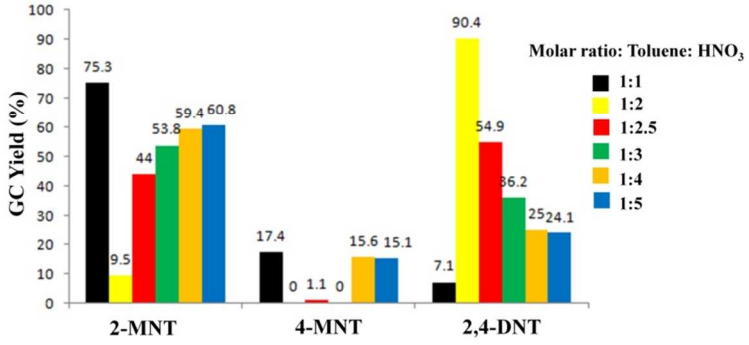

Figure 12. Optimizing of molar ratio of toluene and nitric acid (Reaction conditions: T= 90 °C, solvent-free, catalyst: 15 mol%, time= 3, 1, 1, 1, 0.5, 0.5 h for each molar ratio 1:1 to 1:5 respectively)

As shown in Figure 13, the binary spinel ferrite such as $CuFe_2O_4$, and $CoFe_2O_4$ could not be effective catalysts for dinitration of toluene under solvent-free conditions. The best catalytic activity for the yield and selectivity was observed by increasing the ratio of cobalt element up to 0.5. Homogeneity of the structure of catalyst was destroyed and the yield of 2,4-DNT was decreased to 19.6% with using of high ratio of 0.5, e.g. $Cu_{0.25}Co_{0.75}Fe_2O_4$. Nitration of toluene was also checked in the absence of spinel ferrites so that the selectivity of 2,4-DNT was far from the best conditions. Hence, the influence of spinel ferrites on the distribution of products nitration of toluene was approved with this experiment.

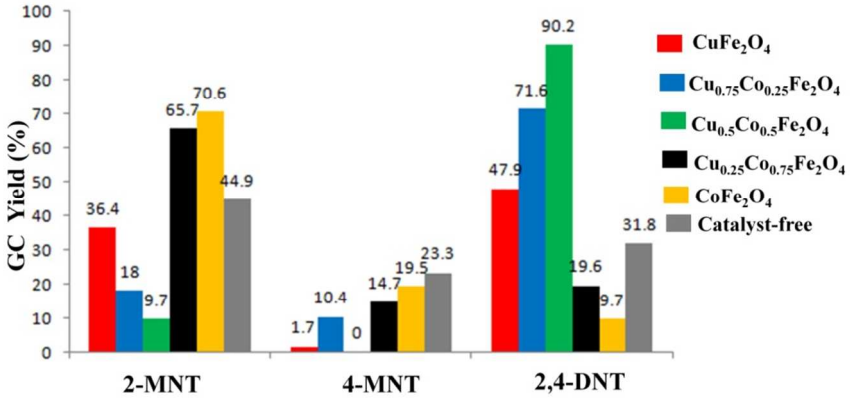

Figure 13. Influence of the type of spinel ferrite on distribution of nitration system (Reaction conditions: toluene: $HNO_3$98%: $Cu_{1-x}Co_xFe_2O_4$= 1:2:0.15, T= 90 °C, solvent-free, time= 4h)

In order to show the best conditions of this study for dinitration of toluene, Figure 14 was depicted. As shown in this Figure, the spinel ferrite $Cu_{0.5}Co_{0.5}Fe_2O_4$, solvent-free, 90 °C, and nitric acid (98%) were the optimum conditions for this study. Additionally, the amount of catalyst and molar ratio of (toluene: nitric acid-98%) were 15 mol% and 1:2, respectively.

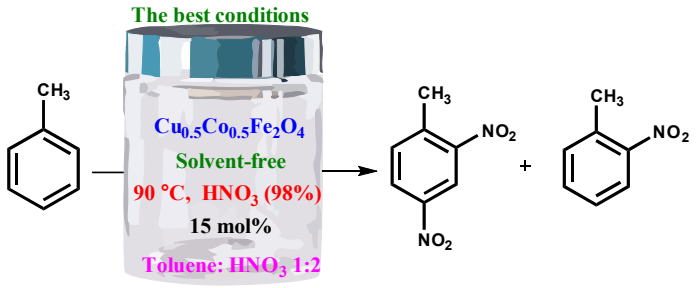

Figure 14. Nitration of toluene under optimum conditions

The plausible mechanism was presented in Figure 15. As shown in Figure 15, the metal ions Fe, Cu, and Co have positive charge and the oxygen ions have negative charge in the cubic spinel ferrite $Cu_{0.5}Co_{0.5}Fe_2O_4$. Therefore, the catalyst accelerates the formation of electrophile NO_2^+ in the corner of the cubic spinel ferrite $Cu_{0.5}Co_{0.5}Fe_2O_4$, which attacks the electron rich *ortho* and

para positions of toluene to produce of 2,4-DNT product. Since the special shape and structure of the $Cu_{0.5}Co_{0.5}Fe_2O_4$ is cubic, the formation of 2,4-DNT is more preference relative to 2,6-DNT. The orientation of catalyst and toluene was also better in solvent free conditions when polar solvent was used.

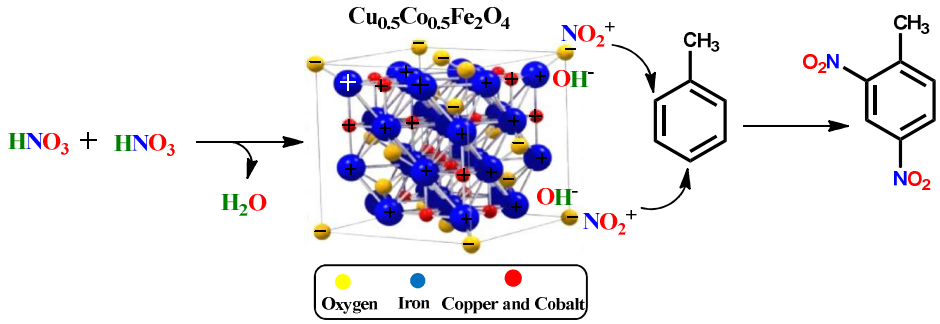

Figure 15. The proposed mechanism for the reaction in the presence of cubic spinel ferrite

4. Conclusion

It was established that the copper and cobalt synergy in $M_{0.5}M'_{0.5}Fe_2O_4$ is an efficient and heterogeneous catalyst for the high regioseletive and green synthesis of 2,4-dinitrotoluene. The use of 1:2:0.15 ratio of toluene: nitric acid: $Cu_{0.5}Co_{0.5}Fe_2O_4$ gives 2,4-DNT in 90.2% yield. 98% Nitric acid is more attractive than 65% nitric acid in terms of double nitration of toluene, and time of the reaction. The best temperature for the nitration of toluene in this protocol was 90 °C when the reaction was performed in any organic solvent. To the best of our knowledge up to date, there is no report on the use of spinel ferrites in the nitration of toluene. The current work obtained the best regioselectivity for the production of 2,4-DNT without the formation of 2,6-DNT. 2,4-DNT compound was also separated from 4-MNT *via* recrystallization in ethanol, while the separation of 2,4-DNT and 2,6-DNT is a hard and intolerable work. Therefore, this protocol

represents an efficient method for the production of 2,4-DNT in the polyurethane industry and double based propellants as precursor and plasticizer, respectively.

Acknowledgement

We gratefully acknowledge the financial support by Malek-ashtar University of Technology (MUT). Also, the authors acknowledge Dr. Farhad Panahi, Dr. Mohsen Golestanzadeh, and Dr. Mojtaba Khorasani for helpful discussions and providing GC chromatograms.

References

1. P. M. Qureshi, S. M. A. Andrabi, A. Saeed and A. Ahmad, *Analytical Proceedings including Analytical Communications*, 1995, **32**, 273-274.
2. J. E. Sawicki, Google Patents, 1983.
3. M. A. Ali, S. S. Y. Chen, H. Cavaye, A. R. G. Smith, P. L. Burn, I. R. Gentle, P. Meredith and P. E. Shaw, *Sen. Actuat. B: Chem.*, 2015, **210**, 550-557.
4. J. Chen, K. Przyuski, R. Roemmele and R. P. Bakale, *Org. Proc. Res. Develop.*, 2013, **18**, 1427-1433.
5. G. Wegener, M. Brandt, L. Duda, J. Hofmann, B. Klesczewski, D. Koch, R. J. Kumpf, H. Orzesek, H. G. Pirkl, C. Six, C. Steinlein and M. Weisbeck, *Appl. Catal. A: General*, 2001, **221**, 303-335.
6. J. A. Brydson, in *Plastics Materials (Sixth Edition)*, ed. J. A. Brydson, Butterworth-Heinemann, Oxford, 1995, pp. 756-787.
7. M. D. Roldán, E. Pérez-Reinado, F. Castillo and C. Moreno-Vivián, *FEMS Microb. Rev.*, 2008, **32**, 474-500.

8. K. Tohru and H. Takahiro, in *Synthesis and Chemistry of Agrochemicals IV*, *J. Am. Chem. Soc.*, 1995, **584**, 15-24.

9. B. Gigante, A. O. Prazeres, M. J. Marcelo-Curto, A. Cornelis and P. Laszlo, *J. Org. Chem.*, 1995, **60**, 3445-3447.

10. X. Peng and H. Suzuki, *Org. Lett.*, 2001, **3**, 3431-3434.

11. H. M. Brennecke and K. A. Kobe, *Indust. Eng. Chem.*, 1956, **48**, 1298-1304.

12. A. Kogelbauer, D. Vassena, R. Prins and J. N. Armor, *Catal. Today*, 2000, **55**, 151-160.

13. K. Smith and G. A. El-Hiti, *Green Chem.*, 2011, **13**, 1579-1608.

14. K. Smith, M. H. Alotaibi and G. A. El-Hiti, *J. Catal.*, 2013, **297**, 244-247.

15. X. Peng, H. Suzuki and C. Lu, *Tetrahedron Lett.*, 2001, **42**, 4357-4359.

16. D. P. Debecker, V. Hulea and P. H. Mutin, *Appl. Catal. A: General*, 2013, **451**, 192-206.

17. H. Tüysüz, E. L. Salabaş, E. Bill, H. Bongard, B. Spliethoff, C. W. Lehmann and F. Schüth, *Chem. Mater.*, 2012, **24**, 2493-2500.

18. J. Shi, *Chem. Rev.*, 2012, **113**, 2139-2181.

19. W. B. Yi and C. Cai, *Synth. Commun.*, 2006, **36**, 2957-2961.

20. P.-C. Wang and M. Lu, *Tetrahedron Lett.*, 2011, **52**, 1452-1455.

21. R. P. Claridge, N. Llewellyn Lancaster, R. W. Millar, R. B. Moodie and J. P. B. Sandall, *J. Chem. Soc., Perkin Trans. 2*, 1999, 1815-1818.

22. D. Vassena, A. Kogelbauer and R. Prins, *Catal. Today*, 2000, **60**, 275-287.

23. *The MAK-Collection for Occupational Health and Safety*, Wiley-VCH Verlag GmbH & Co. KGaA, 2002.

24. D. F. Othmer and H. L. Kleinhans, *Indust. Eng. Chem.*, 1944, **36**, 447-451.

25. J. Adamiak and M. Chmielarek, *J. Indust. Eng. Chem.*, 2015, **27**, 175-181.

26. M. Kong, K. Wang, R. Dong and H. Gao, *Enzyme Microb. Technol.*, 2015, **73–74**, 34-43.

27. W. Zhang, J. Zhang, S. Ren and Y. Liu, *J. Org. Chem.*, 2014, **79**, 11508-11516.

28. J. Green, J. Cao, U. K. Bandarage, H. Gao, J. Court, C. Marhefka, M. Jacobs, P. Taslimi, D. Newsome, T. Nakayama, S. Shah and S. Rodems, *J. Med. Chem.*, 2015, **58**, 5028-5037.

29. K. Smith, M. H. Alotaibi and G. A. El-Hiti, *J. Catal.*, 2013, **297**, 244-247.

30. M. B. Gawande, P. S. Branco and R. S. Varma, *Chem. Soc. Rev.*, 2013, **42**, 3371-3393.

31. P. Dechambenoit and J. R. Long, *Chem. Soc. Rev.*, 2011, **40**, 3249-3265.

32. S. Singh, B. C. Yadav, V. D. Gupta and P. K. Dwivedi, *Mater. Res. Bull.*, 2012, **47**, 3538-3547.

33. J. Yun-Ho, S. Seung-Deok, S. Hyun-Woo, P. Kyung-Soo and K. Dong-Wan, *Nanotech.*, 2012, **23**, 125402.

34. S. Sultana, Rafiuddin, M. Zain Khan and K. Umar, *J. Alloys Compd.*, 2012, **535**, 44-49.

35. R. Fareghi-Alamdari, M. Golestanzadeh and N. Zekri, *J. Chin. Chem. Soc.*, 2014, **61**, 1341-1350.

36. R. Fareghi-Alamdari, Z. Hosseinabadi and M. Khouzani, *J. Chem. Sci.*, 2012, **124**, 827-834.

37. A. Xia, S. Liu, C. Jin, L. Chen and Y. Lv, *Mater. Lett.*, 2013, **105**, 199-201.

38. Y. Pu, X. Tao, J. Zhai and J.-F. Chen, *Mater. Res. Bull.*, 2010, **45**, 616-620.

39. K. Ounnunkad and S. Phanichphant, *Mater. Res. Bull.*, 2012, **47**, 473-477.

40. S. Briceño, H. D. Castillo, V. Sagredo, W. Bramer-Escamilla and P. Silva, *Appl. Surf. Sci.*, 2012, **263**, 100-103.

41. T. Mathew, M. Vijayaraj, S. Pai, B. B. Tope, S. G. Hegde, B. S. Rao and C. S. Gopinath, *J. Catal.*, 2004, **227**, 175-185.

42. A. M. Pachpinde, M. M. Langade, K. S. Lohar, S. M. Patange and S. E. Shirsath, *Chem. Phys.*, 2014, **429**, 20-26.

43. S. Phumying, S. Labuayai, E. Swatsitang, V. Amornkitbamrung and S. Maensiri, *Mater. Res. Bull.*, 2013, **48**, 2060-2065.

44. D. Nandan, P. Sreenivasulu, N. Viswanadham, K. Chiang and J. Newnham, *Dalton Trans.*, 2014, **43**, 12077-12084.

45. T. Şimşek, S. Akansel, Ş. Özcan and A. Ceylan, *Ceram. Int.*, 2014, **40**, 7953-7956.

46. N. Dong, F. He, J. Xin, Q. Wang, Z. Lei and B. Su, *Mater. Lett.*, 2015, **141**, 238-241.

47. Q. Song and Z. J. Zhang, *J. Am. Chem. Soc.*, 2004, **126**, 6164-6168.

48. B. Sreedhar, A. S. Kumar and D. Yada, *Tetrahedron Lett.*, 2011, **52**, 3565-3569.

49. R. Ghahremanzadeh, Z. Rashid, A. H. Zarnani and H. Naeimi, *Appl. Catal. A: General*, 2013, **467**, 270-278.

50. Y. Fang, Y. Liu, W. Deng and J. Liu, *J. Energ. Chem.*, 2014, **23**, 527-534.

51. J. E. Baker, R. Burch and N. Yuqin, *Appl. Catal. A: General*, 1991, **73**, 135-152.

52. D. S. Mathew and R.-S. Juang, *Chem. Eng. J.*, 2007, **129**, 51-65.